

Dynamic Behavior of Planetary Gears

Dr.-Ing. Burkhard Pinnekamp, Dr.-Ing. Michael Heider, and M.Sc. Andreas Beinestingel

Introduction

Besides power density, reliability and efficiency, noise is always an important criterion for a successful gear design. In many theoretical and experimental investigations and papers, the influences and potential remedies were discussed. For example, in (Ref. 6) the importance of a large overlap ratio, achieved by a large helix angle is described as the most important factor for reducing gear noise. In planetary gear systems of high power density and high gear ratio, helical gears create undesirable tilting moments on the planet gears; therefore, spur gears are still preferred for planetary gears—a special challenge with respect to noise. Specifically, the different behavior of planetary gears with sequential and symmetric gear mesh is explained in this paper.

As described (Ref. 10), the variable mesh stiffness along the path of contact in the tooth contact leads to oscillating forces on the shafts and bearings, which are transmitted to the casing. The casing vibrations radiate airborne noise (Fig. 1).

The influence of tooth geometry on the excitation behavior is determined by the geometry parameters, such as profile and overlap ratios, flank modifications and manufacturing deviations. For design to low noise emission, the knowledge of the elastic and dynamic behavior of the transmission system and the excitation mechanisms of the gear mesh is required. Parameters which are useful to evaluate the dynamic behavior of a gear mesh are described in this paper.

The findings of (Ref. 10) are summarized in this paper, further developed and, for sequential gear mesh, applied to a practical example with test stand measurements. Hereby, the theory is

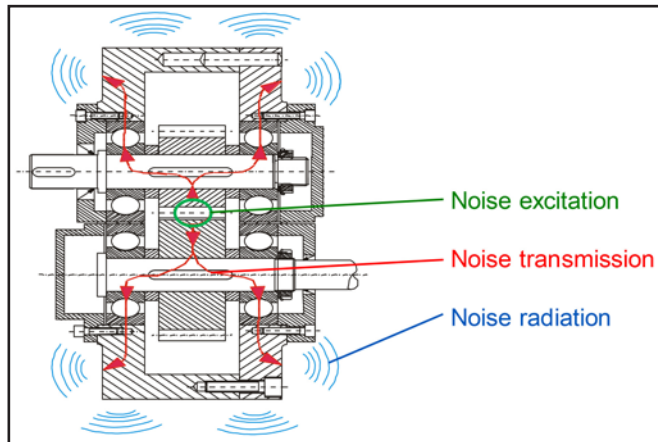


Figure 1 Noise: generation, transmission and radiation.

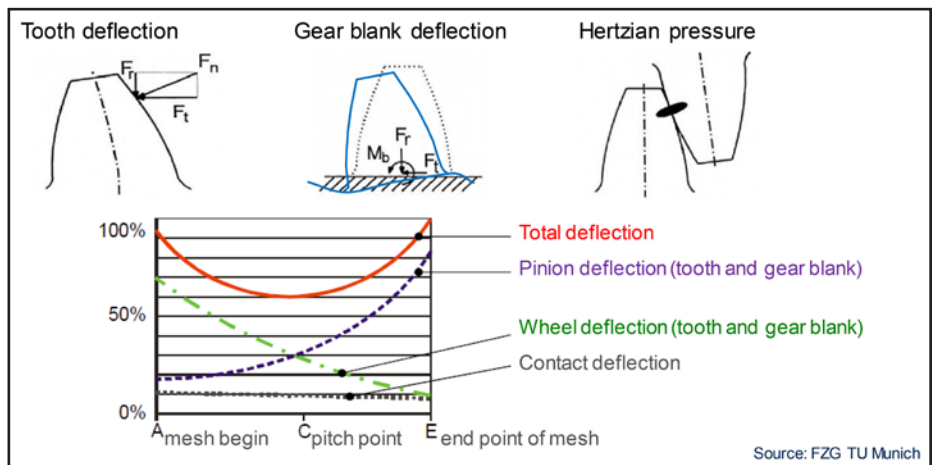


Figure 2 Contributions to single tooth contact deflection along path of contact (Source: FZG TU Munich).

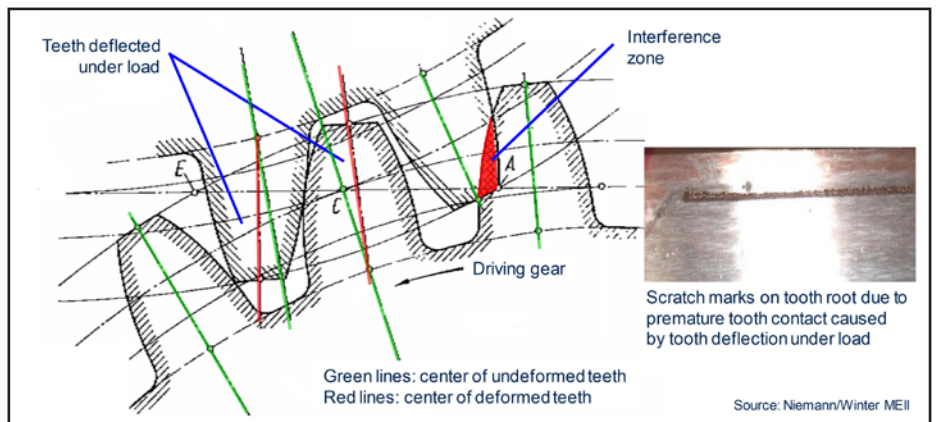


Figure 3 Interference due to tooth deflection under load (Source: Niemann/Winter MEI).

Printed with permission of the copyright holder, the American Gear Manufacturers Association, 1001 N. Fairfax Street, Fifth Floor, Alexandria, VA 22314-1587. Statements presented in this paper are those of the author(s) and may not represent the position or opinion of the American Gear Manufacturers Association.

further sustained on how several variables impact gear noise in parallel shaft and planetary gear trains.

Gear Mesh Excitation

For a cylindrical, involute gear mesh, the main parameters of excitation are:

- Time-varying tooth stiffness
- Deflection of the teeth
- Deviations in tooth geometry
- Deflection of shafts, bearings and casing
- Premature tooth contact under load

Tooth deflection and mesh stiffness.

Single tooth mesh stiffness consists of three components as depicted in Figure 2:

- Tooth deflection due to bending under load
- Bending deflection of the gear blank or gear rim
- Contact deflection of surfaces under Hertzian stress

Even with close to perfectly manufactured gear geometry, due to this elastic deformation under load, the flank position will shift relative to the theoretical unloaded position (Ref.5). There will be interference between the gear teeth with the subsequent, not-yet-loaded gear teeth, which are about to enter the mesh (Fig.3), causing periodic noise excitation. This interference can be compensated for by appropriate profile modification, which only can be optimized for one load level. If not addressed appropriately, the subsequent teeth will come into contact prematurely outside the path of contact (“premature gear mesh”) and may cause stretch marks (Fig.3).

Dynamic excitation. Even with perfect profile modification preventing an interference between the mating gear teeth entering the gear mesh, the total mesh stiffness varies considerably along the path of contact. This is caused by the influences as described in Figure 2 and, moreover, in the change between single and double tooth contact along the path of contact. Especially for spur gears, two indicators for excitation can be derived from this change of stiffness (Fig.4):

- **Transmission error**, which is the static deflection between pinion and wheel under load, ignoring mass acceleration forces, and describes the oscillation of output speed at

constant input speed.

- **Force excitation**, which is the maximum dynamic force created by the transmission error without compensating movement of masses (i.e., rigid masses). It may be used as the force parameter to evaluate the level of excitation, but does not, however, consider the real dynamic system.

Mesh stiffness, transmission error and force excitation are shown (Fig.4) for a spur gear pair without flank corrections. The mesh stiffness (red line) herein is defined from the ideal involute. The transmission error (blue line) represents the angular position difference from uniform transmission. The

effects of excitation can be seen significantly in this curve. Additionally, the force excitation (green curve) represents the mesh force when rolling pinion and wheel are at perfectly constant speed, as defined by the gear ratio. In addition to the time-dependent curves, the referring spectra are shown.

These values can also be used to evaluate influences of deviations or microgeometry modifications; therefore their description in an accurate way is necessary. The curves in Figure 5 (left side) are for a spur gear pair with pitch deviation. The amplitude of harmonics of mesh frequency are high and a low-frequency excitation is added. In Figure

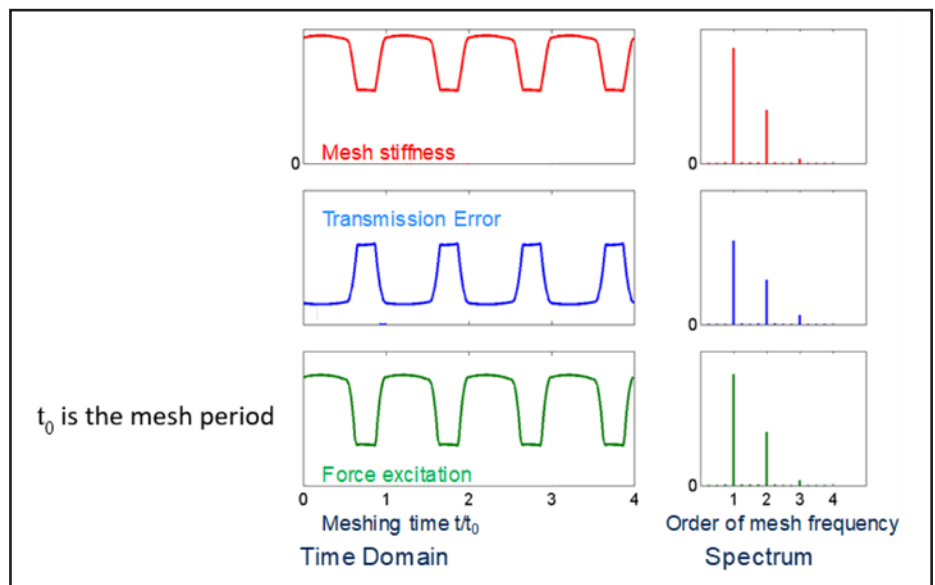


Figure 4 Characteristic parameters for spur gear with unmodified involute profile.

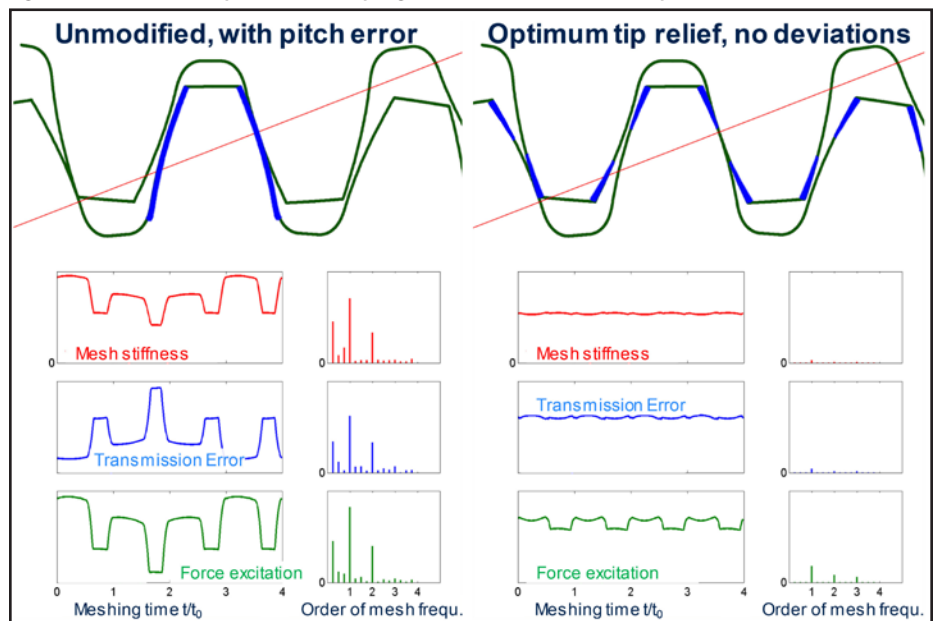


Figure 5 Influence of pitch deviation and profile modification on the characteristic parameters for a spur gear mesh.

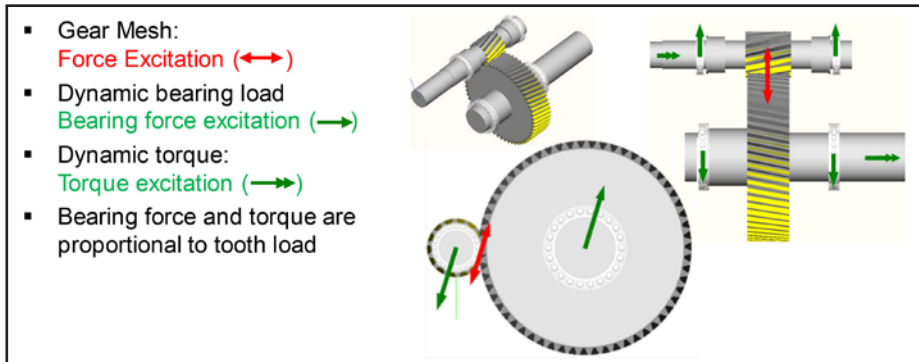


Figure 6 Dynamic excitation in helical gear stage; rotational and lateral dynamic effects are coupled.

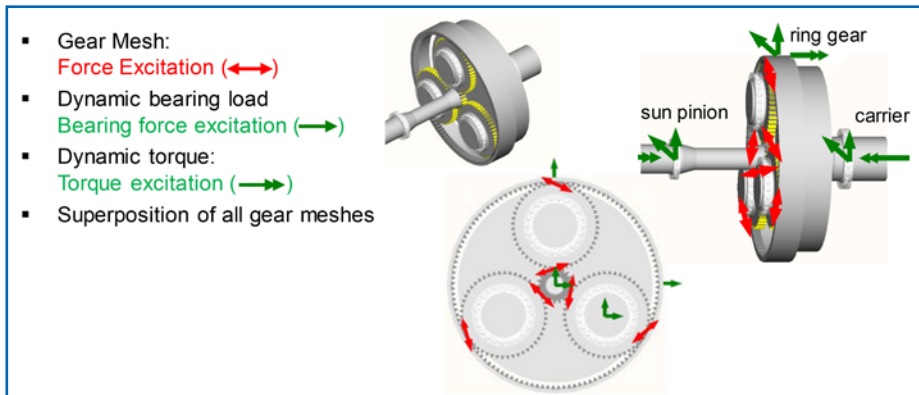


Figure 7 Dynamic excitation in planetary gear stage; rotational and lateral dynamic effects are not coupled.

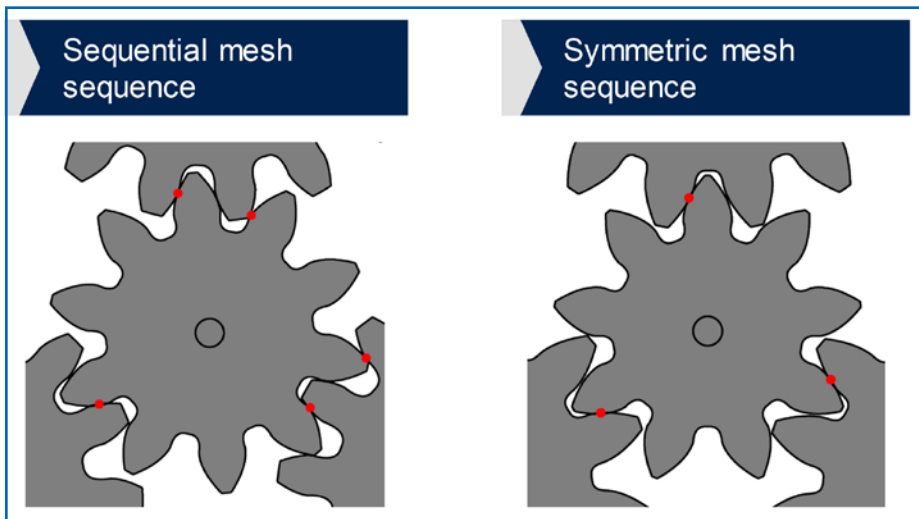


Figure 8 Mesh sequence in planetary gear stage.

5 (right side), the curves for the same mesh are shown without pitch deviation and with optimized profile modification. All values show significant improvements of excitation with considerably smaller amplitudes.

Excitation Modes for Cylindrical Gear Stage and Planetary Gear Stage

For a parallel offset gear stage, one gear mesh is subject to transmission error and force excitation. This excitation causes both oscillating bearing load and shaft torque, where load and torque are synchronous and both proportional to the excitation. Rotational and lateral dynamic effects are therefore coupled (Fig. 6).

This is different with planetary gear stages as the sun pinion is in mesh with multiple planet gears simultaneously. The excitation of all meshes is superposed on the sun pinion. This superposition may be favorable or unfavorable:

- The *lateral excitation* of the sun pinion causing lateral vibrations and dynamic bearing load is determined by the sum of all force vectors of the individual meshes. To keep lateral excitation to a minimum, *all mesh forces should be equal* at any time and hereby fully balanced.
- The *rotational excitation* of the sun pinion causing torsional vibrations is determined by the sum of torque created by all gear meshes. To keep torsional excitation to a minimum, *the scalar sum of all mesh forces should be equal* at any time.

Both requirements are in contradiction; for planetary gears, rotational and lateral dynamic effects are not coupled (Fig. 7).

Influence of Mesh Sequence in Planetary Gear Stages

The result of the superposition of force excitation in the individual gear meshes of a planetary gear stage strongly depends on the phase of the mesh excitations to each other. An important parameter is the mesh sequence which is the phasing between the individual meshes. For equally spaced planets, it can be distinguished between:

- **Symmetric mesh sequence:** number of teeth of the sun pinion is divisible by number of planets. All meshes are at the same point on the path of contact at any time.
- **Sequential mesh sequence:** number of teeth of the sun pinion is not divisible by number of planets. The meshes are at different points on path of contact at any time (Fig. 8).

Planetary gear stage with sequential mesh sequence. Figure 9 shows the force excitation and the torque excitation of the sun pinion for a planetary gear stage with sequential mesh sequence. The individual meshes are distinguished by different colors; they show the typical phase offset for sequential mesh sequence. There are always two meshes in single contact area (low force) and one mesh in double contact area (high force). In the schematic drawings, all radial forces on the sun pinion are shown for the indicated point in time. There is always one force higher than the other two, thus leaving a radial force in alternating directions (black arrows); the total torque, however, is constant at any time.

Planetary gear stage with symmetric mesh sequence. Figure 10 shows the force excitation and the torque excitation of the sun pinion for a planetary gear stage with symmetric mesh sequence. The individual meshes are theoretically shown in the same different colors (Fig. 9). As there is no phase offset, all curves are identical and cannot be distinguished. They show the typical synchronous phase for symmetric mesh sequence. All meshes are either in single contact area (low force) or in double contact area (high force) at the same time. In the schematic drawings, all radial forces on the sun pinion are shown for the indicated point in time. The force vectors always balance to zero; however, the total torque alternates periodically.

Comparison of symmetric and sequential mesh sequence. It can be derived from the statements in the previous paragraphs that either lateral excitation (with symmetric mesh sequence) or torsional excitation (with sequential mesh sequence) can be optimized by just the selection of mesh sequence. The comparison is shown in Figure 11 and Figure 12.

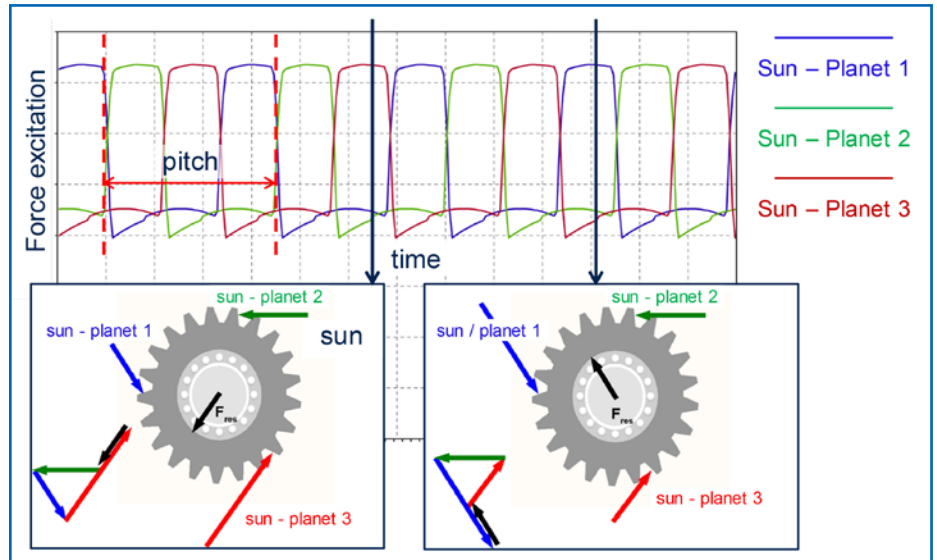


Figure 9 Force excitation of meshes sun-planet (unmodified spur gears); sequential mesh sequence.

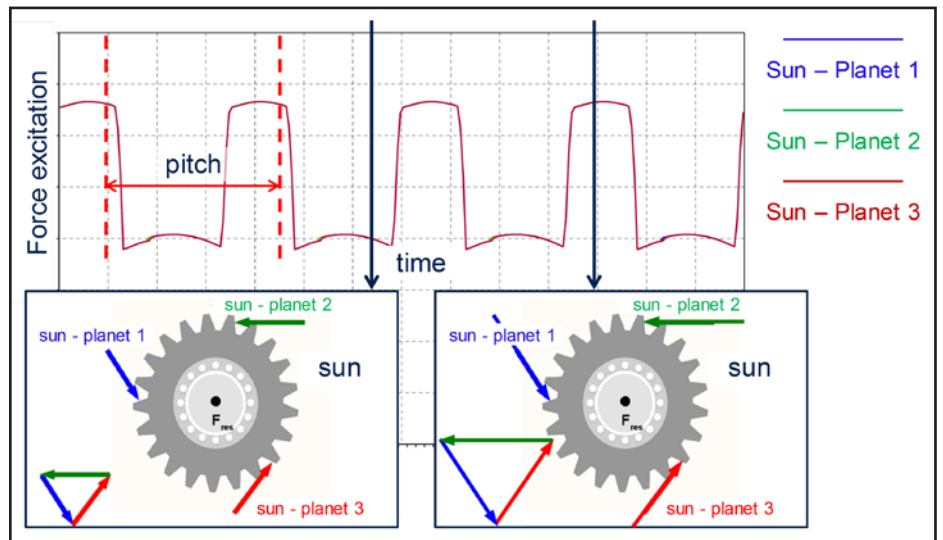


Figure 10 Force excitation of meshes sun-planet (unmodified spur gears); symmetric mesh sequence.

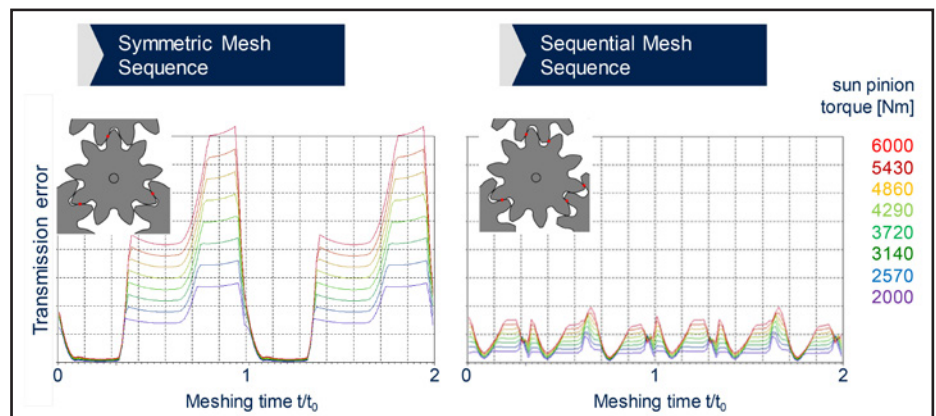


Figure 11 Transmission error between sun and ring gear (unmodified) — torsional excitation.

The only remedy to reduce both excitation modes to a minimum is to reduce the actual transmission error by optimum profile modification as shown on the right side of Figure 5. Profile modification should preferably be done by tip relief on both mating gears. The amount of tip relief depends on tooth deflection and therefore depends on load. Tip relief does not change natural

frequencies.

Practical Example for Optimizing a Planetary Gear

For a practical application, two different sets of sun pinion and planet gears were used on a test bench—one with appropriate profile modification and one without. The different noise excitation levels were validated by measure-

ment of casing vibrations at increasing speed without generator load. The gear is for a 6 MW power plant application where a steam turbine (11,000 rpm) runs a generator (1,500 rpm) via the reduction planetary gear (Fig. 13).

The original gear design started with the typical selection of macrogeometry parameters such as module, number of teeth, contact ratio to match the requirements with respect to specification and load carrying capacity. The gear mesh frequency, f_z , is rated as:

$$f_z = \frac{(n_{sun} - n_{carr}) * z_{sun}}{60^{sec/min}} \quad (1)$$

where

- n_{sun} is the sun pinion speed in rpm
- n_{carr} is the planet carrier speed in rpm
- z_{sun} is the number of teeth of the sun pinion

For the actual application, 23 teeth on the sun pinion result in sequential mesh sequence. With the planet carrier being at a standstill, and an input speed of 11,000 rpm, a tooth mesh frequency of 4,217 Hz is calculated. With this frequency, interference with natural frequencies (from lateral and torsional vibrations calculations) is avoided.

Figure 14 shows the actual test setup, where both gear sets, with and without profile modification were installed for testing. Measurements of casing vibrations were taken and plotted in waterfall diagrams ramping the speed up from zero to 105% of nominal speed without generator load. Figure 15 shows the resulting waterfall diagrams for the modified (left diagram) and unmodified (right diagram) gear set. It can clearly be seen that the overall vibration level is much greater with the unmodified gears—especially the mesh frequency and its second and third orders. This effect is predominant because of the strong lateral excitation for sequential mesh sequence.

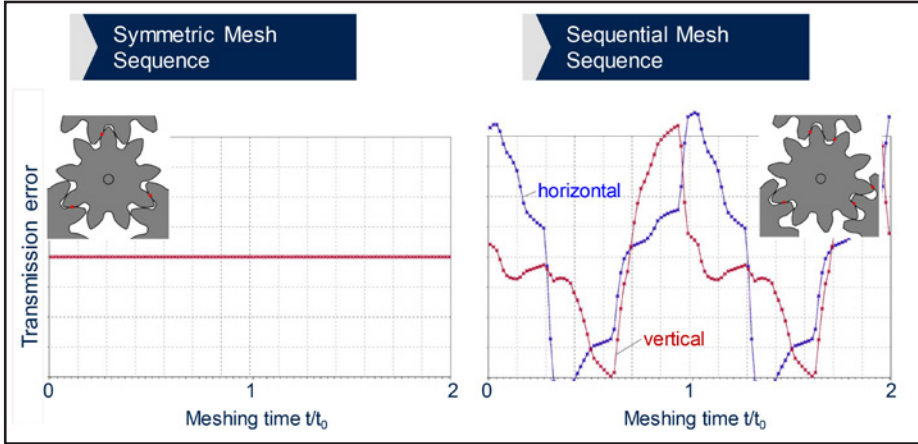


Figure 12 Radial displacement of sun pinion (unmodified) — lateral excitation.

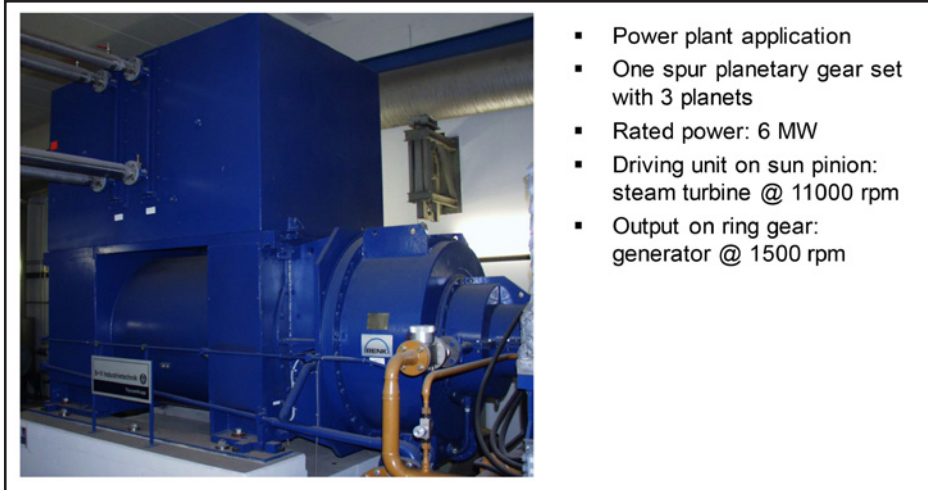


Figure 13 Gear application for testing — main data.

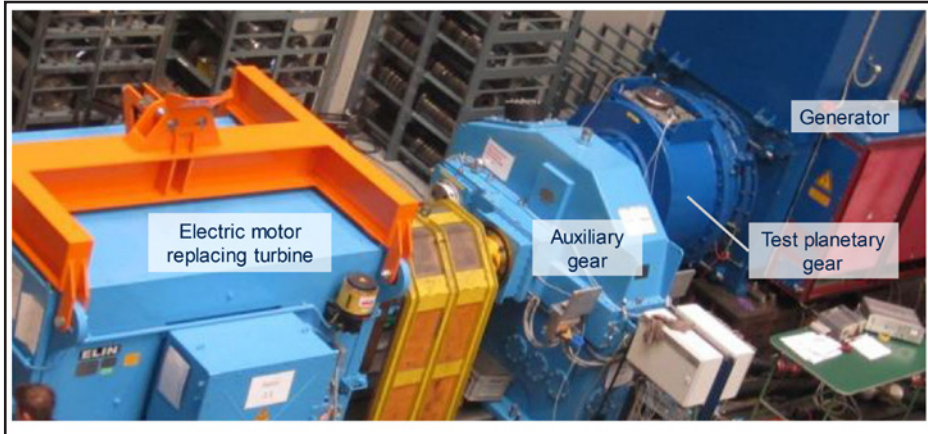


Figure 14 Test setup.

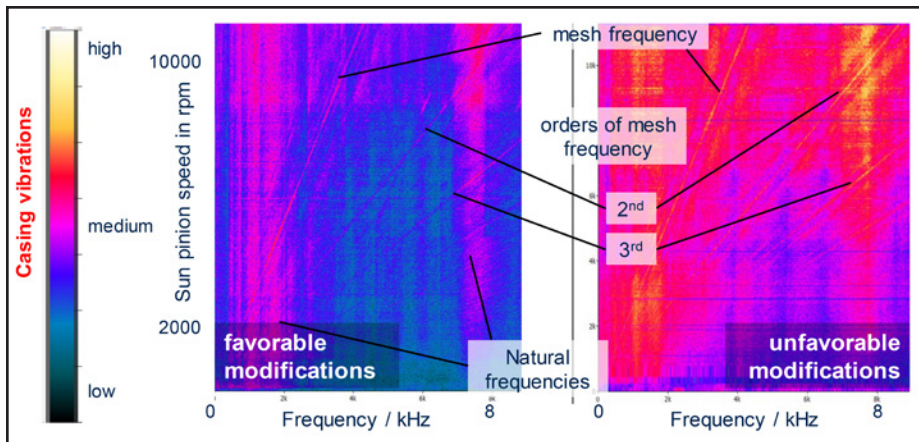


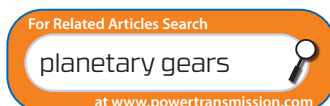
Figure 15 Speed ramp; measurement of casing vibrations.

Conclusions

- Decisive parameters for the dynamic behavior of a gear mesh are transmission error and force excitation.
- Superposition of these parameters for planetary gears (three planets) leads to the following specific aspects:
 - Independent radial load and torque excitation
 - Gear geometry deviations and profile modification have a strong impact on the excitation level
 - Best remedy is low mesh excitation level
- Influence of mesh sequence:
 - For sequential mesh sequence, radial excitation is predominant; choose if torsional vibration excitation needs to be minimized
 - For symmetric mesh sequence, torsional excitation is predominant; choose if lateral vibration excitation needs to be minimized
- Practical example with sequential mesh sequence confirms the impact of profile modification on the vibration excitation level.
- Comparison of sequential and symmetric gear mesh could so far not be validated by testing. This should be done with the next suitable opportunity. **PTE**

For more information.

Questions or comments regarding this paper? Contact the authors at info@renk.biz.



References

1. Oster, P. *Influence of Overlap Ratio on Noise Exciting Level*, Research program of FVA 58/T252, 1985.
2. Palmer, Fuehrer. "Noise Control in Planetary Transmission," SAE Paper No. 770561, April 18-20, 1977.
3. Müller, R. "Vibration and Noise Excitation with Toothed Gears," Dissertation at Technical University, Munich, 1991.
4. Hofmann, D.A., J. Haigh, and Lt. I. Atkins, "The Ultra-Low Noise Gearbox," *Transactions of INEC 2000*, Hamburg, March 2000.
5. Niemann, G. and H. Winter. *Maschinenelemente Band II*, Springer Verlag, Berlin Heidelberg New York (English).
6. Hoppe, F. and B. Pinnekamp. "Challenge and Success Based on Optimized Gear Geometries," *AGMA Fall Technical Meeting*, October 24-26, 2004, Milwaukee, WI.
7. Griggel, T., M. Heider and J. Bihl. FVA-Heft 937: FVA-Forschungsvorhaben 338 V, DZP / DZPopt, DZP Version 5.0 und DZPopt Version 2.0 / *Forschungsvereinigung Antriebstechnik e.V. (FVA)*; Frankfurt/Main, 2010 - *Abschlussbericht*.
8. Heider, M. FVA-Heft 968: FVA-Forschungsvorhaben 292 II, *Anregungsoptimaler Planetenradsatz: Software zur Optimierung des Anregungsverhaltens eines Planetenradsatzes / Forschungsvereinigung Antriebstechnik e.V. (FVA)*. Frankfurt/Main, 2011 - *Abschlussbericht*.
9. Heider, M. "Schwingungsverhalten von Zahnradgetrieben," Dissertation at Technical University, Munich, 2012
10. Heider, M., J. Bihl, M. Otto, B.-R. Hoehn and K. Stahl. "Vibration Excitation of a Planetary Gear Stage," *International Conference on Gears*, Munich, Garching, October 7-9, 2013.
11. Heider, M., B. Pinnekamp and A. Beinstingel. "Planetary Gears: Excitation Modes, Noise and Modifications," *International Conference on Gears*, Munich, September 18-20, 2019.

Dr.-Ing. Burkhard Pinnekamp

earned his degree in mechanical engineering in 1987, and a Ph.D. in 1992 at the Gear Research Center (FZG), Technical University Munich. He continued work at FZG as chief engineer in the field of continuously variable transmission and hybrid car propulsion systems. From 1996 to 1999, he was deputy chief designer with the design department for marine gears at RENK AG, Augsburg. From 1999 to 2001, he headed the design department for industrial gears and, from 2001 to 2004, he led the design department for high-speed gears at RENK AG, Augsburg. From 2004 to 2006, he continued with RENK Corporation, USA, for various marine and industrial gear programs. Since mid-2006, Pinnekamp has served as head of the Central Technology division at RENK AG, Augsburg, focusing on gear calculation, programming, structural and dynamic analyses and innovation management.



Dr.-Ing. Michael Heider

earned a degree mechanical engineering in 2006 and a Ph.D. in 2012 at the Gear Research Center (FZG), Technical University Munich. He continued work at FZG as team leader for gear dynamics and calculation. From 2014-2016, he was senior engineer at the Central Technology Division of RENK AG, Augsburg, focusing on gear calculation, programming, structural and dynamic analyses. Since 2016 Heider has been team leader for calculation at the Central Technology Division for RENK.



Andreas Beinstingel

is a computational engineer for industrial and marine gears with a focus on structural dynamics and acoustics. He holds a bachelor degree in mechanical engineering from Augsburg University of Applied Sciences, and a master degree in computational engineering from Munich University of Applied Sciences. He joined the transmission industry at the beginning of 2015 at RENK AG Augsburg as a software developer in the field of structural mechanics. Since 2018, Beinstingel has also been working as an external Ph.D. student at the Chair of Vibro-acoustics of Vehicles and Machines (VIB) at the Technical University of Munich (TUM). The research partnership between RENK AG Augsburg and TUM includes the investigation of the excitation behavior of involute gears under operating conditions within its mathematical implementation in simulation algorithms.

